Requirement for expression of WW domain containing transcription regulator 1 in bovine trophectoderm development

Shun Saito[†], Shota Yamamura[†], Nanami Kohri, Hanako Bai, Masashi Takahashi, and Manabu Kawahara*

Laboratory of Animal Genetics and Reproduction, Research Faculty of Agriculture, Hokkaido University, Kita-ku, Kita 9, Nishi 9, Sapporo 060-8589, Japan

*Correspondence:

Dr. Manabu Kawahara, PhD

Laboratory of Animal Genetics and Reproduction, Graduate School of Agriculture, Hokkaido University, Sapporo 060-8589, Japan

Tel. & Fax: +81 11 706 2541

E-mail address: k-hara@anim.agr.hokudai.ac.jp

[†]These authors contributed equally to this study.

Abstract

WW domain-containing transcription regulator 1 (WWTR1) is one of the primary effectors in the Hippo pathway, which plays essential roles in cell differentiation into trophectoderm (TE) and inner cell mass cell lineages at the blastocyst stage. However, little is known about the roles of WWTR1 in preimplantation development. The present study aimed to explore the significance of WWTR1 expression in preimplantation development using an mRNA knockdown (KD) system in bovine embryos. We first quantitated WWTR1 expression at protein and mRNA levels from fertilization to blastocyst stage. WWTR1 proteins gradually shifted from extranuclear localization during the 16-cell stage to nuclear localization by morula stage. *WWTR1* mRNA expression was also transiently upregulated at the 16-cell stage. *WWTR1* KD efficiently repressed WWTR1 expression at protein and mRNA levels. The *WWTR1* KD embryos developed to the blastocyst stage at rates equivalent to those of controls, but TE cell numbers were significantly decreased. Representative TE-expressed genes, including *CDX2* and *IFNT* were also significantly decreased in *WWTR1* KD blastocysts. These results provide the first demonstration that WWTR1 expression is responsible for normal TE cell development in preimplantation embryos.

Keywords: embryo, blastocyst, trophectoderm, cattle, Hippo pathway, differentiation

Abbreviations

TE, trophectoderm; ICM, inner cell mass;YAP1, yes-associated protein 1; TEAD4, TEA domaintranscription factor 4; CDX2, caudal type homeobox 2; LATS1/2, large tumor suppressor 1/2; SOX2, SRY-box transcription factor 2; CCN2, cellular communication network factor 2; OCT4, POU class 5 homeobox 1 (POU5F1)

Introduction

How one fertilized zygote gives rise to a variety of cell types and becomes a complex adult body is one of the most intriguing puzzles in biology. The fertilized zygote repeatedly undergoes cleavage, increasing the cell number. Embryonic cells then gradually establish characteristic transcriptional profiles adapted to their microenvironment, migrating as the mature to play specialized roles in specific tissues throughout the complex adult body [1]. Such self-organization is driven by adaptive gene regulatory networks. TE cells, a group of cells that undergo the earliest cell-fate decision from undifferentiated embryonic cells, express a key transcription factor CDX2. The TE cells form the placenta, while the ICM cells that do not express CDX2 give rise to the embryo proper. This cell lineage specification is called the first cell-fate decision. The timing of stabilization of this cell fate varies among species [2,3]. The Hippo pathway activates a phosphorylation cascade in response to changes in microenvironment surrounding each cell. This pathway appears to be a conserved mechanism among many species for orchestrating the first cell-fate decision (to TE or ICM cells) of blastocysts [4,5].

The Hippo pathway components, TEAD4, YAP1, and WWTR1, also called TAZ, are expressed in morula and blastocyst stage embryos in many mammals [5–7].

When the Hippo pathway is activated in the ICM, both WWTR1 and YAP1 are phosphorylated, preventing translocation into the nucleus, resulting in cytoplasmic localization. By contrast, the Hippo pathway is inactivated in the TE. WWTR1 and YAP1 are not phosphorylated and can interact with nuclear TEAD4 to induce TE-specific genes including, *CDX2* [8]. Thus, subcellular localization of the last two effectors, YAP1 and WWTR1, is critical for producing the asymmetry between TE and ICM within a blastocyst through interaction with TEAD4, which is localized to TE nuclei [2,4,6]. To date, although YAP1 has been well studied, the functions of WWTR1 have not been elucidated in mammalian embryos [5,7,9].

While YAP1 is highly conserved among species [10], WWTR1 appeared much later than YAP1 in vertebrate evolution [11]. Bovine YAP1 (Accession No: XP_024831476) and WWTR1 (Accession No: NP_001179976) proteins are approximately 60% homologous, spanning multiple functional domains. Both proteins contain WW domains that interact with LATS1/2 to phosphorylate WWTR1 and YAP1 when the Hippo pathway is activated [12]. Each protein also contains several unique domains. YAP1 uniquely contains an SH3-binding motif and an N-terminal proline-rich region [8] . WWTR1 uniquely contains a phosphodegron that is directly phosphorylated by GSK3β [13]. In accord with these structural differences, there are overt differences

in the phenotypes of knockout (KO) mice for each gene. YAP1 KO mice display embryonic lethal with failure of yolk sac vasculogenesis at day (E) 8.5 [14]. Whereas 20% of WWTR1 KO remain viable, although they develop renal cysts and lung emphysema [15–17]. Nevertheless, WWTR1 and YAP1 have been regarded to be functionally redundant in mammalian early embryos, therefore the role of YAP1 in preimplantation development has been studied in detail, but that of WWTR1 has not.

In the present study, we first determined WWTR1 expression dynamics at protein and mRNA levels during bovine preimplantation development. We then performed *WWTR1* knockdown (KD) by microinjection of *WWTR1* short-hairpin RNA into presumptive zygotes, and assessed the effects of *WWTR1* KD on blastocyst formation. The TE cell number of the WWTR1 KD blastocysts was significantly decreased compared with control embryos. Thus, these results provide first demonstration that WWTR1 plays significant roles particular to TE development in bovine embryos in mammalian blastocysts.

Materials and Methods

Preparation of in vitro fertilized embryos

Bovine embryos were prepared via *in vitro* fertilization as previously described [18,19]. Briefly, cumulus-oocyte complexes (COCs) were aspirated from 3–8-mm follicles in ovaries retrieved from a slaughterhouse. COCs including intact cumulus cells were cultured at 38.5°C in a humidified atmosphere with 5% CO_2 and air for 20 to 22 h in 100-mL droplets of TCM199 (Gibco, Grand Island, NY) containing 10 mM cysteamine (Sigma-Aldrich, St. Louis, MO), 10% (v/v) fetal bovine serum (PAA Laboratories, Pasching, Austria), 0.5 mg/mL follicle-stimulating hormone (Kyoritsu Seiyaku Corp., Tokyo, Japan), 100 U/mL penicillin (Nacalai Tesque, Inc., Kyoto, Japan), and 100 U/mL streptomycin (Nacalai Tesque, Inc.) covered with liquid paraffin oil. Oocytes were then transferred to Brackett and Oliphant (BO) medium [20] containing 2.5 mM theophylline (Wako Pure Chemical Industries, Ltd., Osaka, Japan). Frozen-thawed semen was centrifuged at 600 X *g* for 7 min in BO medium, and spermatozoa were added to the COCs at a final concentration of 5×10^6 cells/mL. After 12 h of incubation, presumptive *in vitro*-fertilized zygotes were denuded by pipetting, and cultured at 38.5°C in a humidified atmosphere with 5% CO_2 using synthetic oviduct fluid (SOF) medium supplemented with 10 mg/mL insulin (Sigma-Aldrich), 1 mg/mL

polyvinyl alcohol (Sigma-Aldrich), and 10 mM cysteamine. Embryos were used for microinjection immediately after denuding. Rates of cleavage and blastocyst formation were assessed on days 2 and 8 of *in vitro* culture, respectively.

Immunofluorescence and confocal microscopy

Primary antibodies included rabbit anti-WWTR1 (V386) (1:300, CAT No.#4883, Cell Signaling Technology, USA), rabbit anti-CDX2 (1:200, ab76541; Abcam), and rabbit anti-SOX2 (1:1500, ab92494; Abcam). The secondary antibodies used were as follows: Alexa Fluor 488 Goat anti-rabbit IgG Cross-Adsorbed (A11008, polyclonal, 1:400, Invitrogen Tokyo, Japan) and Alexa Fluor 555 goat anti-rabbit IgG (A21428, polyclonal, 1:400, Invitrogen). Oocytes and embryos were fixed with 4% (w/v) paraformaldehyde (PFA; Wako Pure Chemical Industries) in PBS for 60 min, then permeabilized for 60 min with 0.2% (v/v) Triton X-100 in PBS. Next, oocytes and embryos were blocked for 45 min with blocking buffer; Blocking One (1:5; Nacalai Tesque, Inc.) diluted in 0.05% (v/v) Tween 20 in PBS. Thereafter, oocytes or embryos were incubated in blocking buffer containing the primary antibody for 8 h at 20–22°C. After washing 5 X 10 minutes in PBS containing 0.1% (v/v) Triton X-100 and 0.3% (w/v) bovine serum albumin (Sigma-Aldrich), oocytes and embryos were incubated for

30 min at room temperature with secondary antibody diluted to 1:400 in 0.01%(v/v) Tween 20 in PBS. Nuclei were counterstained with 25 mg/mL Hoechst 33342 (Sigma-Aldrich) prepared in 0.2% (w/v) polyvinyl alcohol in PBS. Fluorescence signals were visualized using a Leica: TCS SP5 confocal laser-scanning microscope (Leica, Wetzlar, Germany).

Quantitative PCR

Total RNA from five oocytes or embryos per biological replicate was isolated using a ReliaPrep RNA Cell Miniprep System (Promega Corporation, Madison, WI, USA), following the manufacturer's instructions. Syntheses of embryonic cDNA were conducted using a ReverTra Ace qPCR RT Master Mix (Toyobo, Osaka, Japan). Quantitative PCR (qPCR) was performed after preparing reaction mixtures in THUNDERBIRD SYBR qPCR Mix (Toyobo). Primer sets used for analyses are listed in Table 1. Relative expression levels of *WWTR1* and *YAP1* were determined after normalization using the geometric mean of internal standard genes (*GAPDH*, *ACTB*, and *YWHAZ*) to eliminate differences among developmental stages in expression of internal standard genes. *WWTR1* expression in *WWTR1* KD experiments was calculated relative to transcription of one internal control, *H2AFZ* (H2A histone family member Z)

in each sample, in accord with a previous study [19]. The experiments were performed in triplicate.

Microinjection of the WWTR1 *shRNA expression vector*

Construct preparation for RNA interference by microinjection into presumptive zygotes was performed as previously described [21]. An shRNA containing antisense/sense regions, a 23-bp loop (5- AAGTTAAACATGAATAAACATTT) and a 6-bp terminator element (5-TTTTTT), was designed to target nucleotides 1679-1701 of *WWTR1* mRNA (Accession No.; XM_005201825.4). The dsDNA was ligated downstream of the U6 promoter into the pBAsi/mU6 Neo vector (Stratagene, CA, USA). The *WWTR1* mRNA-targeting shRNA (*WWTR1* shRNA) expression vector (pBAsi/mU6/WWTR1) was prepared using an EZgene EndoFree Plasmid Miniprep Kit II (Biomiga, Inc., San Diego, CA). pBAsi/mU6 Neo plasmid lacking the *WWTR1* shRNA insert (empty vector) [21–23] was used as a control for embryo injection. Twelve hours after insemination, synthesized *WWTR1* shRNA or empty-vector control DNA (diluted to a final concentration of 10 ng/mL with SOF medium) was injected into the cytoplasm of denuded zygotes using a FemtoJet injection device (Eppendorf, Hamburg, Germany). These presumptive zygotes were cultured to examine the effect of

KD on embryonic development from 12 hours post fertilization to blastocyst stage.

Statistical Analysis

All experimental data are presented as mean ± standard errors of the mean (SEM). In the data on both *WWTR1* expression levels and rates of development to the blastocyst stage, statistically significant differences were compared using repeated-measures ANOVA followed by Tukey's *post hoc* tests. All other data were statistically analyzed using unpaired Student's *t* test. R software (Comprehensive R Archive Network, https://cran.r-project.org/) was used for all statistical analyses. $P < 0.05$ was considered statistically significant.

Results

Bovine WWTR1 expression at protein and mRNA levels during early embryonic development.

We first determined WWTR1 protein expression patterns by immunostaining GV oocytes and embryos ranging from 12 hours post fertilization to blastocyst stage (Fig. 1A). WWTR1 proteins were predominantly localized to the cytoplasm in GV and MII oocytes, and in 2C embryos. At 4C and 8C stages, WWTR1 proteins were present in the cytoplasm and in the nuclei. At 16C stage, fluorescent staining of WWTR1 protein was observed more strongly in the nuclei than in the cytoplasm in some blastomeres. At both the morula and blastocyst stages, WWTR1 proteins were exclusively localized to the nuclei in the outer cells.

We next investigated *WWTR1* mRNA expression dynamics in GV oocytes through blastocyst stage embryos (Fig. 1B). Until the 8C stage, WWTR1 expression remained at low levels. By contrast, *WWTR1* expression was transiently upregulated at the 16C stage ($P < 0.05$). *WWTR1* expression was again downregulated at morula and blastocyst stages. This transient increase in *WWTR1* expression might be associated with a shift in WWTR1 protein localization from cytoplasm to nucleus at the 16C stage.

Effect of *WWTR1* KD on bovine preimplantation development

We examined the significance of *WWTR1* expression during bovine preimplantation development by KD of *WWTR1* mRNA expression. Relative *WWTR1* mRNA abundance was significantly lower in *WWTR1* KD blastocysts than in controls ($P < 0.05$) (Fig. 2A). Furthermore, an obvious reduction in WWTR1 protein throughout *WWTR1* KD blastocysts was confirmed by immunostaining (Fig. 2B). Cleavage and blastocyst formation rates in *WWTR1* KD embryos were similar to those of the controls (Fig. 2C). These results demonstrate that *WWTR1* KD does not affect rates of preimplantation development in cattle.

Effect of *WWTR1* KD on bovine TE formation.

To explore the effect of *WWTR1* KD on bovine TE formation, we performed CDX2 immunostaining (Fig. 3A). A clear reduction in fluorescent signal detecting CDX2 protein was observed in *WWTR1* KD blastocysts (Fig. 3A). We next carried out SOX2 immunostaining to discriminate ICM cells from the other cells in the blastocysts. The SOX2 expression pattern in *WWTR1* KD blastocysts was similar to that in control blastocyst (Fig. 3B). The number of SOX2 negative TE cells was significantly decreased in the *WWTR1* KD blastocysts (Fig. 3C). However, the number of SOX2 positive ICM

cells did not differ between *WWTR1* KD and control blastocysts (Fig. 3C). These results indicate that the reduction in total cell number in *WWTR1* KD blastocysts is due to failure of TE formation rather than that of ICM formation.

Effect of *WWTR1* KD on TE/ICM differentiation-associated genes.

We next examined the effect of *WWTR1* KD on differentiation-associated gene expression to genetically characterize TE and ICM [20]. According to qPCR analyses, expression levels of four representative TE-expressed genes, *CDX2*, *TEAD4, IFNT* and *CCN2* were significantly decreased in *WWTR1* KD blastocysts ($P < 0.05$) (Fig. 4). No significant differences were observed in expression levels of the ICM-expressed genes, *NANOG* and *OCT3/4* (Fig. 4). Hence, these results reinforced failure to form the TE in *WWTR1* KD blastocysts (Fig. 3C).

Discussion

Formations of TE and ICM cell lineages requires inactivated and activated states of the Hippo pathway in the inner and outer cells, respectively. In the outer cells, YAP1 and WWTR1 enter the nucleus, activating TE-expressed genes through interaction with TEAD4. Thus, the presence or absence of nuclear localization for these two effectors determines the TE vs ICM cell fate in early embryos. Expression of WWTR1 during preimplantation development has not been as well characterized that of its paralog, YAP1 [5,7,9]. Here, we attempted to clarify WWTR1 expression dynamics at protein and mRNA levels, and the role of *WWTR1* expression in TE development toward blastocyst formation using a gene-expression KD system.

WWTR1 proteins were detectable throughout preimplantation development. In stages from GV oocyte to 2C embryo, WWTR1 proteins were predominantly localized to the cytoplasm. At 4C and 8C stages, equivalent amounts of WWTR1 protein were localized to both the cytoplasm and the nucleus. From the 16C stage, the outer blastomeres showed nuclear WWTR1 localization. According to previous study, YAP1 protein localization patterns were different from those of WWTR1 protein. In the 16C stage, YAP1 protein started to localize to the nucleus in a part of the cells [9]. As nuclear localization of YAP1 proteins is required for their intervention in transcriptional

regulation, nuclear YAP1 localization might play role in early development prior to the 8C stage, differing from WWTR1 protein [9].

WWTR1 mRNA expression was transiently upregulated at the 16C stage, when an obvious translocation of protein into the nucleus was observed. As activation of zygotic genome transcription starts around the 16C stage in bovine embryos [24], activation of WWTR1 expression at mRNA and protein levels during embryonic development might be coordinated with zygotic genome activation.

To explore the role(s) of *WWTR1* expression in preimplantation development, we investigated development rates and TE/ICM cell allocation in *WWTR1* KD embryos. Knockdown of *WWTR1* mRNA did not impair preimplantation development up to the blastocyst stage, as did *TEAD4* KD [25]. *WWTR1* KD blastocysts formed morphologically normal blastocoel; however, their TE cell numbers were reduced compared with those of controls. As WWTR1 is one of the primary effectors (as is YAP1) in the Hippo pathway that regulates the first cell segregation decision, cell differentiation toward the TE cell lineage might be inhibitted during blastocyst formation. *YAP1* KD blastocysts also show decreased TE cell numbers [10]. Unlike *WWTR1* KD, *YAP1* KD decreased ICM cell numbers. Although the procedure for KD was different from that in the present study, this dissimilarity in KD effects on each cell lineage possibly reflects a

functional difference between WWTR1 and YAP1. WWTR1 expression would be specifically essential for TE proliferation.

In addition to TE cell proliferation, expression levels of representative TE-expressed genes, *CDX2*, *TEAD4*, *CCN2*, and *IFNT*, were downregulated in *WWTR1* KD blastocysts. Reduced TE cell number is probably not the reason for reduced TE-expressed gene expression because CDX2 protein expression was clearly repressed in *WWTR1* KD blastocysts (Fig. 3A). Initiation of *CDX2* gene expression requires inactivation of the Hippo pathway by localization of WWTR1 to the TE nuclei where it interacts with TEAD4, as does YAP1 [4]. This WWTR1-TEAD4 interaction is quantitatively reduced by *WWTR1* KD. Consequently, the TE cells in *WWTR1* KD blastocysts could not maintain a TE cell-specific transcriptional profile, as evidenced by downregulation of the pregnancy recognition factor *IFNT* specific to ruminant TE cells [26]. CCN2 is reported to be a direct *WWTR1* target gene in human cells [27]. *CCN2* downregulation in *WWTR1* KD blastocysts indicates that *CCN2* is also a *WWTR1* target genes in bovine embryos. This might downregulate *TEAD4* because *CCN2* and *TEAD4* reciprocally regulate each other's expression in bovine blastocysts [25]. *TEAD4* downregulation might be due to *CDX2* downregulation in *WWTR1* KD blastocysts because TEAD4 is an essential transcription factor for *CDX2* expression [7].

There was no significant difference in ICM cell numbers between control and *WWTR1* KD blastocysts (Fig. 3C). Furthermore, the expression levels of two potent ICM markers, *OCT3/4* and *NANOG*, in *WWTR1* blastocysts were also equivalent to those in controls (Fig. 4). Notably, *YAP1* KD blastocysts displayed *NANOG* downregulation but did not display significant decrease in *CDX2* expression, unlike *WWTR1* KD blastocysts [10]. Interaction between YAP1 and TEAD family proteins also contributes to mouse embryonic stem cell pluripotency [28]. Therefore, our results suggest that bovine WWTR1 and YAP1 regulate significantly overlapping transcription programs in preimplantation development but WWTR1 also mediates more specific functions underlying TE differentiation in bovine embryos.

In conclusion, the present study has elucidated WWTR1 expression dynamics at protein and mRNA levels and the significance of WWTR1 expression during preimplantation development. Unlike YAP1, WWTR1 specifically directs TE cell differentiation in bovine blastocysts. Further analyses of how WWTR1 contributes to the first cell-fate decision would help understand more precise molecular mechanisms in preimplantation development.

Acknowledgements

We thank the Genetics Hokkaido Association for their donation of frozen bull spermatozoa. We are also grateful to NICHIRO CHIKUSAN CO., LTD., and the Hokkaido Hayakita meat inspection center for providing bovine ovaries.

Funding

This work was supported by a Grant-in-Aid for Scientific Research (B) (grant number 18H02321) from the Japan Society for the Promotion of Science.

References

[1] E. Posfai, I. Rovic, A. Jurisicova, The mammalian embryo's first agenda: Making trophectoderm, Int. J. Dev. Biol. 63 (2019) 157–170. https://doi.org/10.1387/ijdb.180404ep.

[2] N. Kohri, H. Akizawa, S. Iisaka, H. Bai, Y. Yanagawa, M. Takahashi, M. Komatsu, M. Kawai, M. Nagano, M. Kawahara, Trophectoderm regeneration to support full-term development in the inner cell mass isolated from bovine blastocyst, J. Biol. Chem. 294 (2019) 19209–19223. https://doi.org/10.1074/jbc.RA119.010746.

[3] D.K. Berg, C.S. Smith, D.J. Pearton, D.N. Wells, R. Broadhurst, M. Donnison, P.L. Pfeffer, Trophectoderm Lineage Determination in Cattle, Dev. Cell. 20 (2011) 244–255. https://doi.org/10.1016/j.devcel.2011.01.003.

[4] N. Nishioka, K. ichi Inoue, K. Adachi, H. Kiyonari, M. Ota, A. Ralston, N. Yabuta, S. Hirahara, R.O. Stephenson, N. Ogonuki, R. Makita, H. Kurihara, E.M. Morin-Kensicki, H. Nojima, J. Rossant, K. Nakao, H. Niwa, H. Sasaki, The Hippo Signaling Pathway Components Lats and Yap Pattern Tead4 Activity to Distinguish Mouse Trophectoderm from Inner Cell Mass, Dev. Cell. 16 (2009) 398–410. https://doi.org/10.1016/j.devcel.2009.02.003.

[5] C. Gerri, A. McCarthy, G. Alanis-Lobato, A. Demtschenko, A. Bruneau, S. Loubersac, N.M.E. Fogarty, D. Hampshire, K. Elder, P. Snell, L. Christie, L. David, H. Van de Velde, A.A. Fouladi-Nashta, K.K. Niakan, Initiation of a conserved trophectoderm program in human, cow and mouse embryos, Nature. 587 (2020). https://doi.org/10.1038/s41586-020-2759-x.

[6] N. Nishioka, S. Yamamoto, H. Kiyonari, H. Sato, A. Sawada, M. Ota, K. Nakao, H. Sasaki, Tead4 is required for specification of trophectoderm in pre-implantation mouse embryos, Mech. Dev. 125 (2008) 270–283. https://doi.org/10.1016/j.mod.2007.11.002.

[7] C. Yu, S.Y. Ji, Y.J. Dang, Q.Q. Sha, Y.F. Yuan, J.J. Zhou, L.Y. Yan, J. Qiao, F. Tang, H.Y. Fan, Oocyte-expressed yes-associated protein is a key activator of the early zygotic genome in mouse, Cell Res. 26 (2016) 275–287. https://doi.org/10.1038/cr.2016.20.

[8] S. Piccolo, S. Dupont, M. Cordenonsi, The biology of YAP/TAZ: Hippo signaling and beyond, Physiol. Rev. 94 (2014) 1287–1312. https://doi.org/10.1152/physrev.00005.2014.

[9] V.M. Negrón-Pérez, P.J. Hansen, Role of yes-associated protein 1, angiomotin, and mitogen-activated kinase kinase 1/2 in development of the bovine blastocyst,

Biol. Reprod. 98 (2018) 170–183. https://doi.org/10.1093/biolre/iox172.

[10] A. Sebe-Pedrs, Y. Zheng, I. Ruiz-Trillo, D. Pan, Premetazoan Origin of the Hippo Signaling Pathway, Cell Rep. 1 (2012) 13–20. https://doi.org/10.1016/j.celrep.2011.11.004.

[11] J.H. Hong, E.S. Hwang, M.T. McManus, A. Amsterdam, Y. Tian, R. Kalmukova, E. Mueller, T. Benjamin, B.M. Spiegelman, P.A. Sharp, N. Hopkins, M.B. Yaffe, TAZ, a transcriptional modulator of mesenchymal stem cell differentiation, Science (80-.). 309 (2005) 1074–1078. https://doi.org/10.1126/science.1110955.

[12] R. Yagi, L.F. Chen, K. Shigesada, Y. Murakami, Y. Ito, A WW domain-containing Yes-associated protein (YAP) is a novel transcriptional co-activator, EMBO J. 18 (1999) 2551–2562. https://doi.org/10.1093/emboj/18.9.2551.

[13] W. Huang, X. Lv, C. Liu, Z. Zha, H. Zhang, Y. Jiang, Y. Xiong, Q.Y. Lei, K.L. Guan, The N-terminal phosphodegron targets TAZ/WWTR1 protein for SCF β-TrCP-dependent degradation in response to phosphatidylinositol 3-kinase inhibition, J. Biol. Chem. 287 (2012) 26245–26253. https://doi.org/10.1074/jbc.M112.382036.

[14] E.M. Morin-Kensicki, B.N. Boone, M. Howell, J.R. Stonebraker, J. Teed, J.G. Alb, T.R. Magnuson, W. O'Neal, S.L. Milgram, Defects in Yolk Sac

Vasculogenesis, Chorioallantoic Fusion, and Embryonic Axis Elongation in Mice with Targeted Disruption of Yap65, Mol. Cell. Biol. 26 (2006) 77–87. https://doi.org/10.1128/mcb.26.1.77-87.2006.

[15] Y. Tian, R. Kolb, J.-H. Hong, J. Carroll, D. Li, J. You, R. Bronson, M.B. Yaffe, J. Zhou, T. Benjamin, TAZ Promotes PC2 Degradation through a SCFβ-Trcp E3 Ligase Complex, Mol. Cell. Biol. 27 (2007) 6383–6395. https://doi.org/10.1128/mcb.00254-07.

[16] R. Makita, Y. Uchijima, K. Nishiyama, T. Amano, Q. Chen, T. Takeuchi, A. Mitani, T. Nagase, Y. Yatomi, H. Aburatani, O. Nakagawa, E. V. Small, P. Cobo-Stark, P. Igarashi, M. Murakami, J. Tominaga, T. Sato, T. Asano, Y. Kurihara, H. Kurihara, Multiple renal cysts, urinary concentration defects, and pulmonary emphysematous changes in mice lacking TAZ, Am. J. Physiol. - Ren. Physiol. 294 (2008) 542–553. https://doi.org/10.1152/ajprenal.00201.2007.

[17] Z. Hossain, S.M. Ali, L.K. Hui, J. Xu, P.N. Chee, K. Guo, Z. Qi, S. Ponniah, W. Hong, W. Hunziker, Glomerulocystic kidney disease in mice with a targeted inactivation of Wwtr1, Proc. Natl. Acad. Sci. U. S. A. 104 (2007) 1631–1636. https://doi.org/10.1073/pnas.0605266104.

[18] A. Aono, H. Nagatomo, T. Takuma, R. Nonaka, Y. Ono, M. Kawahara,

Dynamics of intracellular phospholipid membrane organization during oocyte maturation and successful vitrification of immature oocytes retrieved by ovum pick-up in cattle, Theriogenology. 79 (2013) 1146–1152. https://doi.org/10.1016/j.theriogenology.2013.02.009.

[19] H. Nagatomo, S. Kagawa, Y. Kishi, T. Takuma, A. Sada, Y. Abe, Y. Wada, M. Takahashi, T. Kono, Transcriptional wiring for establishing cell lineage specification at the blastocyst stage in cattle, Biol. Reprod. 88 (2013) 1–10. https://doi.org/10.1095/biolreprod.113.108993.

[20] B.G. Brackett, G. Oliphant, Capacitation of rabbit spermatozoa in vitro, Biol. Reprod. 274 (1975) 260–274.

[21] H. Akizawa, H. Nagatomo, H. Odagiri, N. Kohri, N. Yamauchi, Y. Yanagawa, M. Nagano, M. Takahashi, M. Kawahara, Conserved roles of fibroblast growth factor receptor 2 signaling in the regulation of inner cell mass development in bovine blastocysts, Mol. Reprod. Dev. 83 (2016) 516–525. https://doi.org/10.1002/mrd.22646.

[22] W.F. Li, Q. Ou, H. Dai, C.A. Liu, Lentiviral-mediated short hairpin RNA knockdown of MTDH inhibits cell growth and induces apoptosis by regulating the PTEN/AKT pathway in hepatocellular carcinoma, Int. J. Mol. Sci. 16 (2015)

19419–19432. https://doi.org/10.3390/ijms160819419.

[23] T. Andey, S. Marepally, A. Patel, T. Jackson, S. Sarkar, M. O'Connell, R.C. Reddy, S. Chellappan, P. Singh, M. Singh, Cationic lipid guided short-hairpin RNA interference of annexin A2 attenuates tumor growth and metastasis in a mouse lung cancer stem cell model, J. Control. Release. 184 (2014) 67–78. https://doi.org/10.1016/j.jconrel.2014.03.049.

[24] R.E. Frei, G.A. and Schultz, R.B. Church, Qualitative quantitative changes in protein synthesis, J. Reprod. Infertil. 86 (1989) 637–641.

[25] H. Akizawa, K. Kobayashi, H. Bai, M. Takahashi, S. Kagawa, H. Nagatomo, M. Kawahara, Reciprocal regulation of TEAD4 and CCN2 for the trophectoderm development of the bovine blastocyst, Reproduction. 155 (2018) 563–571.

[26] K. Imakawa, R. V. Anthony, M. Kazemi, K.R. Marotti, H.G. Polites, R.M. Roberts, Interferon-like sequence of ovine trophoblast protein secreted by embryonic trophectoderm, Nature. 330 (1987) 377–379. https://doi.org/10.1038/330377a0.

[27] H. Zhang, C.Y. Liu, Z.Y. Zha, B. Zhao, J. Yao, S. Zhao, Y. Xiong, Q.Y. Lei, K.L. Guan, TEAD transcription factors mediate the function of TAZ in cell growth and epithelial-mesenchymal transition, J. Biol. Chem. 284 (2009) 13355–

13362. https://doi.org/10.1074/jbc.M900843200.

[28] I. Lian, J. Kim, H. Okazawa, J. Zhao, B. Zhao, J. Yu, A. Chinnaiyan, M.A. Israel, L.S.B. Goldstein, R. Abujarour, S. Ding, K.L. Guan, The role of YAP transcription coactivator in regulating stem cell self-renewal and differentiation, Genes Dev. 24 (2010) 1106–1118. https://doi.org/10.1101/gad.1903310.

Figure legends

Figure 1. Bovine WWTR1 expression at the protein and mRNA levels during preimplantation development. **A**: Immunostaining for the WWTR1 proteins in germinal vesicle (GV), MII oocytes (MII), 2-cell (2C), 8C, 16C, morula (M) and blastocyst (B) embryos. Nuclear DNA was counterstained by Hoechst staining. Green: WWTR1; blue: DNA. Scale bar = 50 μm. **B**: Relative expression levels of the *WWTR1* mRNA from the GV oocyte stage to the blastocyst stage. Three housekeeping genes, *GAPDH*, *ACTB* and *YWHAZ*, were used as internal controls for quantitative PCR. Values are represented as means ± SEM. An asterisk means statistically significant difference ($P < 0.05$).

Figure 2. Validation of *WWTR1* KD by shRNA microinjection and its effect on developmental rates until the blastocyst stage. **A**: *WWTR1* mRNA abundance was determined using quantitative PCR. Three independent experiments were performed. Empty: Embryos that the parent vector without the *WWTR1* shRNA insert was microinjected. Approximately 20–40 embryos were used for *WWTR1* KD and control (Empty) in each experiment. Values are represented as means± SEM. An asterisk means statistically significant difference ($P < 0.05$). **B**: Immunostaining for WWTR1 at the

blastocyst stage. Nuclear DNA was counterstained by Hoechst staining. Green: WWTR1; blue: DNA. Scale bar = 100 μm. **C**: Effect of *WWTR1* KD on embryonic development until the blastocyst stage. Uninjected: n = 87 (white); Empty: n = 163 (gray); *WWTR1* KD: n = 166 (green). Three independent experiments were performed. Values are represented as means ± SEM.

Figure 3. Effect of *WWTR1* KD on bovine TE and ICM formations. A: Immunostaining for CDX2 at the blastocyst stage. CDX2 protein is displayed in green; nuclei are in blue. Scale bar = 100 μm. **B**: Immunostaining for SOX2 at the blastocyst stage. SOX2 protein is displayed in red; nuclei are in blue. Scale bar = 100 μm. **C**: Allocations to the ICM and TE in the *WWTR1* KD and control blastocysts. SOX2 was used as a ICM marker and SOX2 negative cells were counted as TE cells. The number of cells positive for each cell marker was counted. Values are represented as means ± SEM. An asterisk means statistically significant difference ($P < 0.05$).

Figure 4. Effect of *WWTR1* KD on TE/ICM-associated gene expression. The relative expression levels of 4 TE-associated genes, *CDX2*, *IFNT*, *TEAD4*, and *CCN2*, and 2 ICM-associated genes, *NANOG* and *OCT3/4*, were compared between the *WWTR1* KD and

control blastocysts. Data were normalized to *H2AFZ* (H2A histone family member Z) mRNA abundance as an internal control. Three independent experiments were replicated. Values are represented as means ± SEM. An asterisk means statistically significant difference (P <0.05).

A

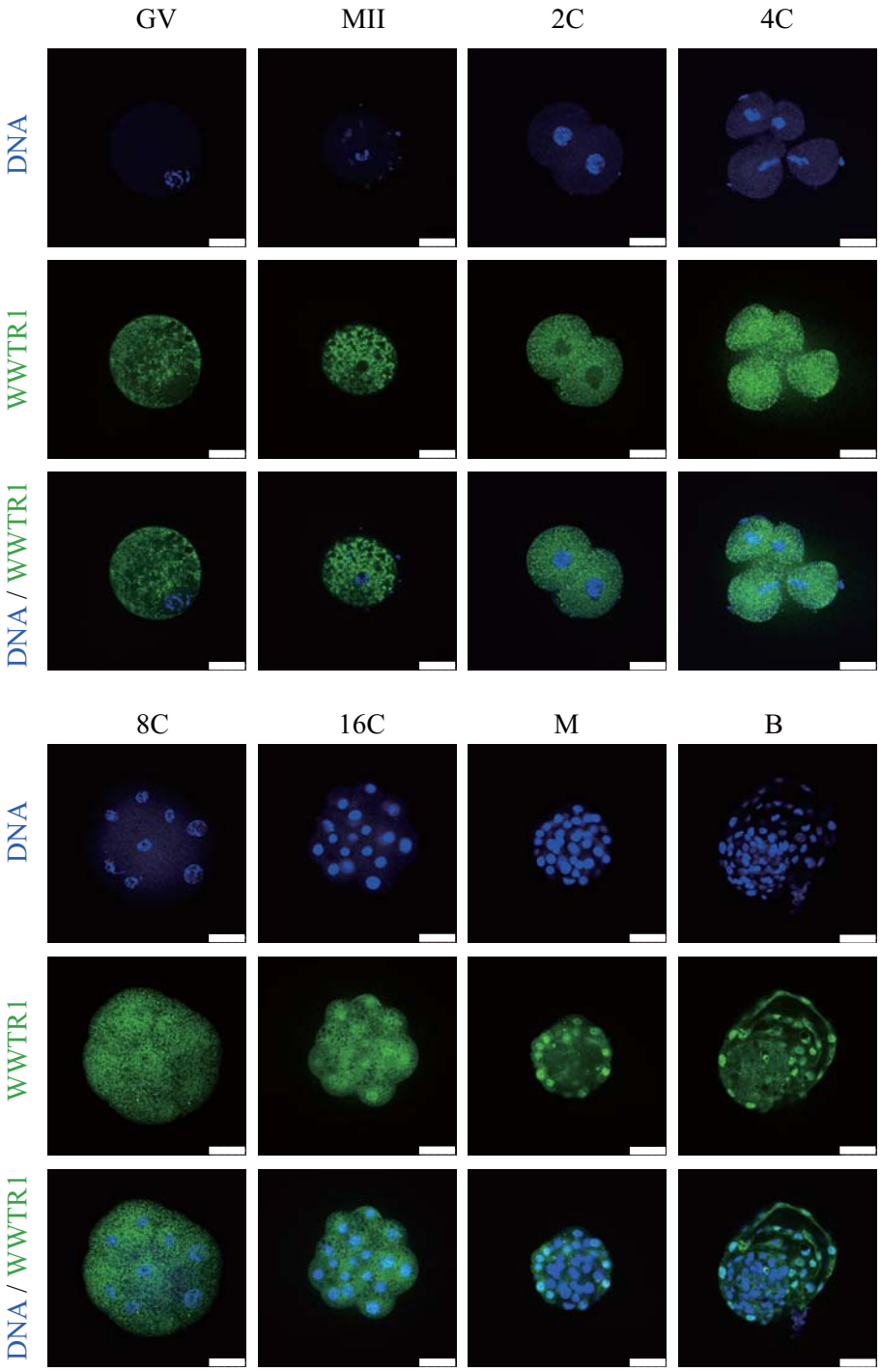
GV
MII
2C
4C
DNA
WWTR1
DNA / WWTR1
8C
16C
M
B
DNA
WWTR1
DNA / WWTR1

B

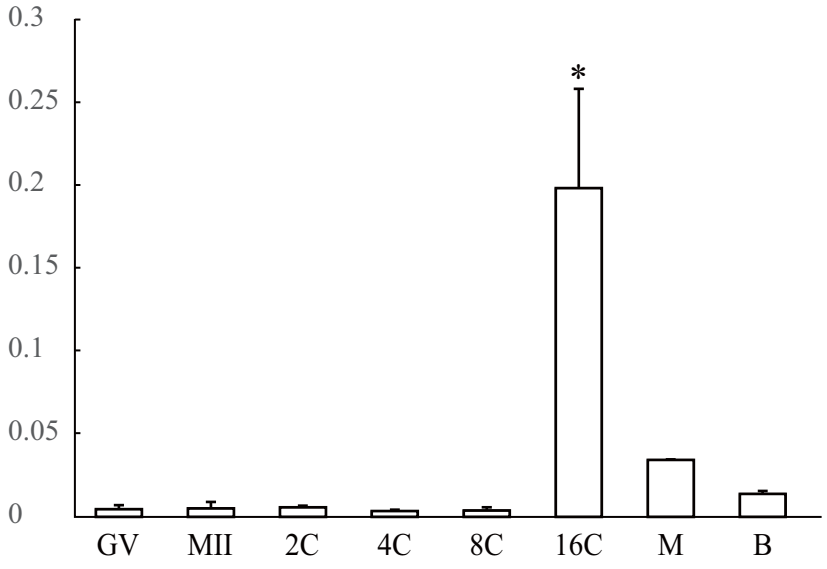
0.3
0.25
0.2
0.15
0.1
0.05
0
*
GV
MII
2C
4C
8C
16C
M
B

A

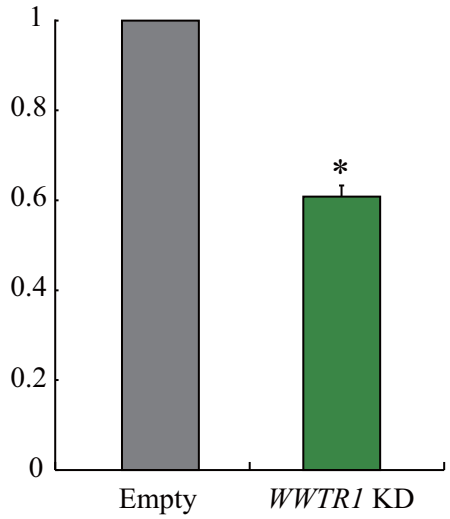
1
0.8
0.6
0.4
0.2
0
*
Empty
WWTR1 KD

B

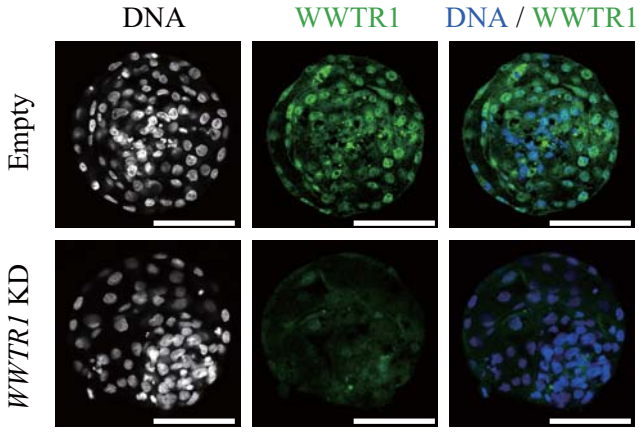
DNA
WWTR1
DNA / WWTR1
Empty
WWTR1 KD

C

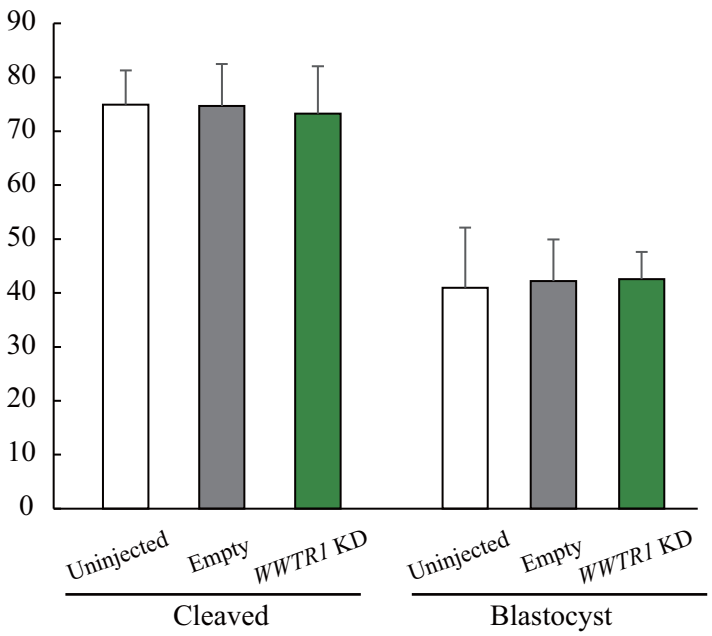
90
80
70
60
50
40
30
20
10
0
Uninjected
Empty
WWTR1 KD
Uninjected
Empty
WWTR1 KD
Cleaved
Blastocyst

A

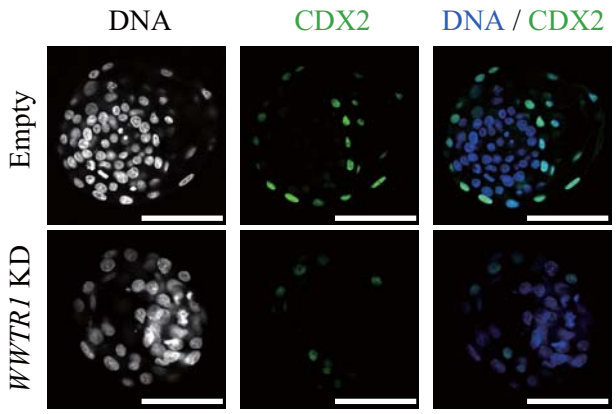
DNA
CDX2
DNA / CDX2
Empty
WWTR1 KD

B

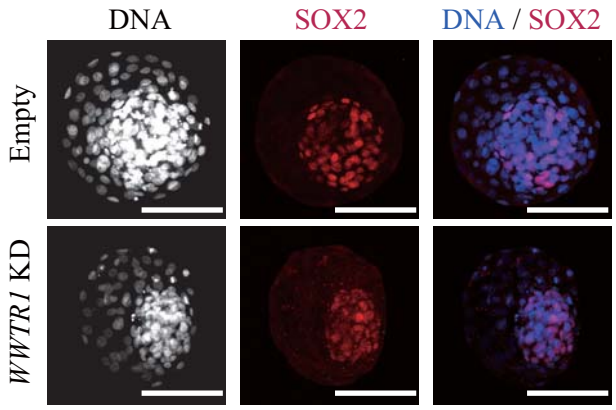
DNA
SOX2
DNA / SOX2
Empty
WWTR1 KD

C

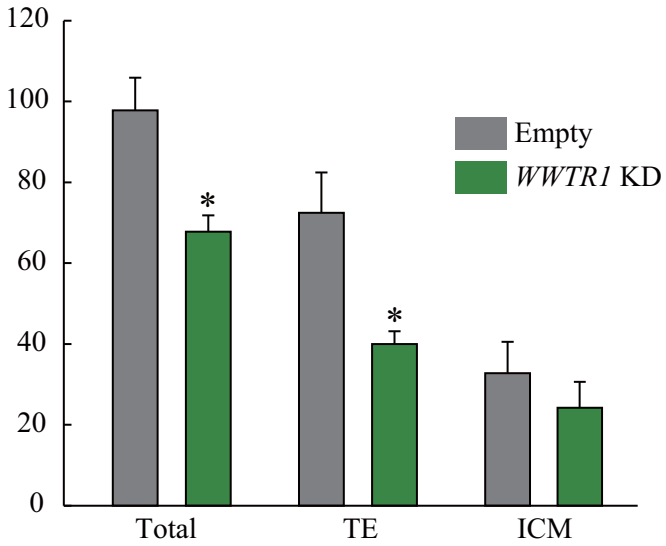
120
100
80
60
40
20
0
*
*
Empty
WWTR1 KD
Total
TE
ICM

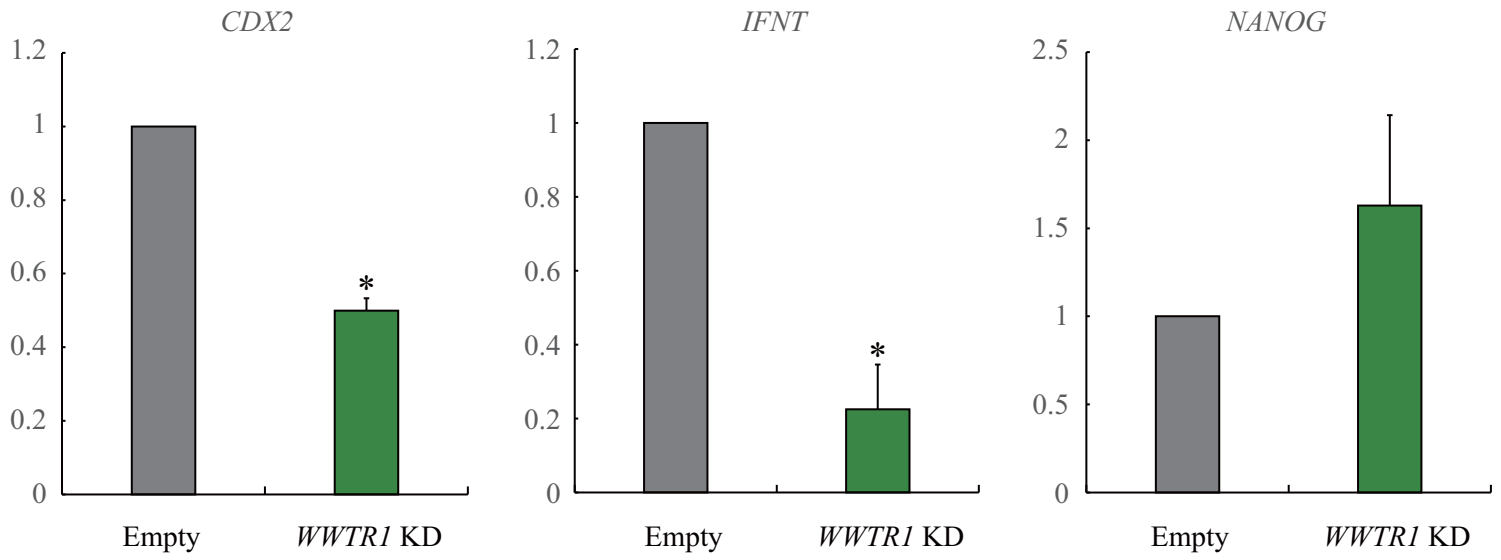
CDX2
1.2
1
0.8
0.6
0.4
0.2
0
*
Empty
WWTR1 KD
IFNT
1.2
1
0.8
0.6
0.4
0.2
0
*
Empty
WWTR1 KD
NANOG
2.5
2
1.5
1
0.5
0
Empty
WWTR1 KD

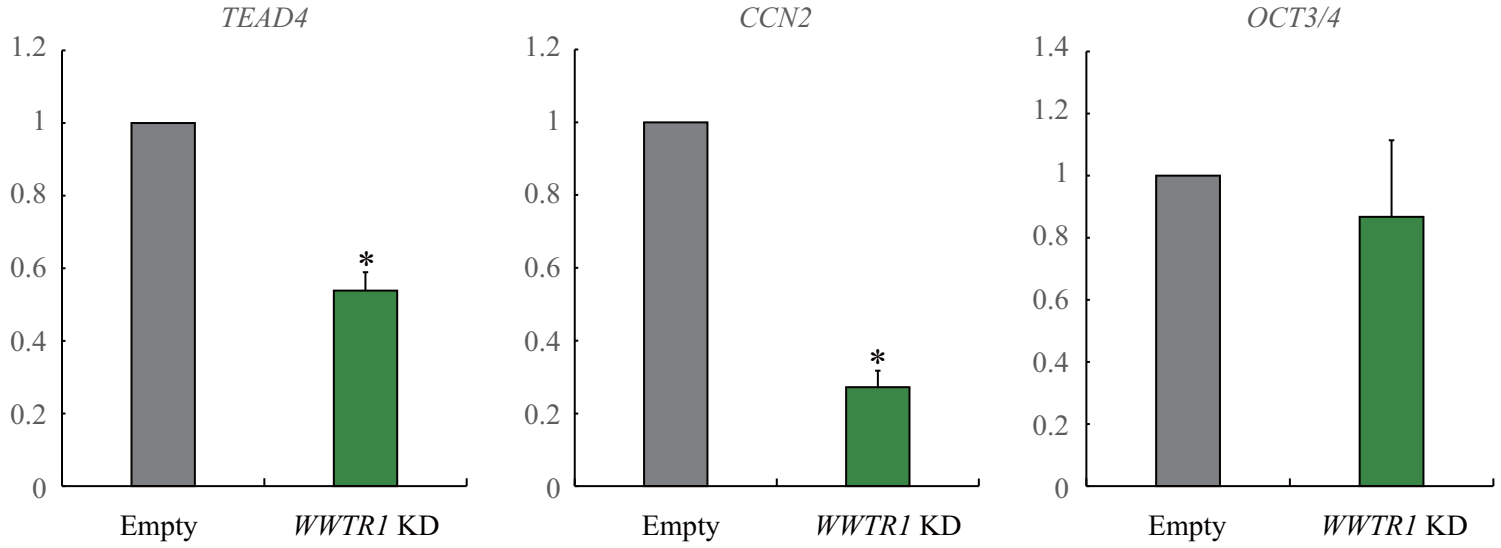
TEAD4
1.2
1
0.8
0.6
0.4
0.2
0
*
Empty
WWTR1 KD
CCN2
1.2
1
0.8
0.6
0.4
0.2
0
*
Empty
WWTR1 KD
OCT3/4
1.4
1.2
1
0.8
0.6
0.4
0.2
0
Empty
WWTR1 KD

Table 1. Primer sets for the quantitative RT-PCR analysis

Gene	Accession number	Primer sequence (5'-3')	Annealing temperture	Product length (bp)
WWTR1	NM_001193047.1	F: TATCATTCGAGGGAGCAGAG R: TCAAGAAAATCAGGGAAACG	67	175
TEAD4	XM_010805630.3	F: GGCAAGATGTATGGTCGGAA R: TGCCTGATCCTTTAGCTTGG	62	150
CDX2	NM_001206299.1	F: GCCACCATGTACGTGAGCTAC R: ACATGGTATCCGCCGTAGTC	58	140
CCN2	NM_174030.2	F: CAAGCAGCTGAGCGAGTTGT R: TGGTACACAGTTCCTCCGAAA	62	150
IFNT	NM_001031765.1	F: CTACTGATGGCCTTGGTGCT R: GTCCTTCTGGAGCTGGTCAC	52	204
NANOG	XM_024992001.1	F: CTCGCAGACCCAGCTGTGTG R: CCCTGAGGCATGCCATTGCT	58	198
OCT3/4	NM_174580.3	F: ACATGTGTAAGCTGCGGCCC R: CTTTCGGGCCTGCACAAGGG	58	107
H2AFZ	NM_174809.2	F: AGAGCCGGTTTGCAGTTCCCG R: TACTCCAGGATGGCTGCGCTGT	58	116
GAPDH	NM_001034034.2	F: ATGCTGGTGCTGAGTATGTAGTGG R: AGAAGCAGGGATGATATTCTGGGC	53	365
ACTB	NM_173979.3	F: GGGACGACATGGAGAAGATC R: CCAGAGGCATACAGGGACAG	51	202
YWHAZ	NM_174814.2	F: TTGGAGGGTCGTCTCCAGTA R: TGCAACCTCAGCCAAGTAGC	65	226